integrating viruses (~0.01 to 0.1%) and is probably due to the fact that many cells do not maintain viral expression long enough to trigger entry into a state sustained by endogenous pluripotency factors (*24*, *25*). This conclusion is supported by qPCR analysis for adenoviral gene expression, which is gradually lost in dividing fibroblasts (fig. S8). It should be informative to test whether the low efficiency of adenoviral reprogramming can be increased by the use of chemical compounds as has been reported for retroviral reprogramming (*26*–*28*).

DNA content analysis showed that 3 out of 13 (or about 23%) of the 13 adeno-iPS lines were tetraploid, which is not seen in iPS cells produced with retro- or lentiviral vectors (fig. S9 and Table 1). We speculate that adenoviral reprogramming either induces cell fusion or, alternatively, selects for rare tetraploid cells pre-existing in the starting cell populations. Indeed, it has been shown that the frequency of polyploid hepatocytes increases with age (*29*).

Our results demonstrate the generation of iPS cells without the use of integrating viruses by employing either a combination of adenoviruses and an inducible transgene or adenoviruses alone. Our work supports the claim that insertional mutagenesis is not required for in vitro reprogramming, and it provides a platform for studying the biology of iPS cells lacking viral integrations. For example, it should now be possible to assess if iPS cells and ES cells are equivalent at the molecular and functional levels. This comparison has not been possible so far because viral transgenes are expressed at low levels in iPS cells and their progeny, which may affect their molecular signatures, as well as their differentiation behavior and developmental potential. If human iPS cells can be generated without genome-integrating viruses, these cells may allow for the generation of safer patient-specific cells and thus could have important implications for cell therapy. Before translating these observations into a therapeutic setting, however, it will be important to assess if human iPS cells generated without viral integration are indeed as potent as human ES cells.

References and Notes

1. K. Takahashi, S. Yamanaka, *Cell* **126**, 663 (2006).
2. M. Stadtfeld, K. Brennand, K. Hochedlinger, *Curr Biol* (2008).
3. J. Hanna *et al*., *Cell* **133**, 250 (2008).
4. S. Eminli, J. Utikal, K. Arnold, R. Jaenisch, K. Hochedlinger, *Stem Cells*, published online 17 June 2008, in press.
5. N. Maherali *et al*., *Cell Stem Cell* **3**, 340 (2008).
6. N. Maherali *et al*., *Cell Stem Cell* **1**, 55 (2007).
7. W. E. Lowry *et al*., *Proc. Natl. Acad. Sci. U.S.A.* **105**, 2883 (2008).
8. K. Okita, T. Ichisaka, S. Yamanaka, *Nature* **448**, 313 (2007).
9. K. Takahashi *et al*., *Cell* **131**, 861 (2007).
10. M. Wernig *et al*., *Nature* **448**, 318 (2007).
11. I. H. Park *et al*., *Nature* **451**, 141 (2008).
12. J. Yu *et al*., *Science* **318**, 1917 (2007).
13. M. Wernig *et al*., *Proc. Natl. Acad. Sci. U.S.A.* **105**, 5856 (2008).
14. J. Hanna *et al*., *Science* **318**, 1920 (2007).
15. R. G. Hawley, *Mol. Ther.* **16**, 1354 (2008).
16. O. Kustikova *et al*., *Science* **308**, 1171 (2005).
17. T. Aoi *et al*., *Science* **321**, 699; published online 14 February 2008 (10.1126/science.1154884).
18. Materials and methods are available as supporting material on *Science* Online.
19. K. Hochedlinger, Y. Yamada, C. Beard, R. Jaenisch, *Cell* **121**, 465 (2005).
20. Q. Li, M. A. Kay, M. Finegold, L. D. Stratford-Perricaudet, S. L. Woo, *Hum. Gene Ther.* **4**, 403 (1993).
21. S. Yamada *et al*., *Endocr. J.* **53**, 789 (2006).
22. A. Harui, S. Suzuki, S. Kochanek, K. Mitani, *J. Virol.* **73**, 6141 (1999).
23. N. Louis, C. Evelegh, F. L. Graham, *Virology* **233**, 423 (1997).
24. T. Brambrink *et al*., *Cell Stem Cell* **2**, 151 (2008).
25. M. Stadtfeld, N. Maherali, D. T. Breault, K. Hochedlinger, *Cell Stem Cell* 10.1016/j.stem.2008.02.001 (2008).
26. D. Huangfu *et al*., *Nat. Biotechnol.* **26**, 795 (2008).
27. T. S. Mikkelsen *et al*., *Nature* **454**, 49 (2008).
28. Y. Shi *et al*., *Cell Stem Cell* **2**, 525 (2008).
29. S. Gupta, *Semin. Cancer Biol.* **10**, 161 (2000).

30. We thank H. Hock for critical comments on the manuscript and L. Prickett and K. Folz-Donahue for expert help with flow cytometry. We are especially grateful to J. Lee of the Harvard Gene Therapy Initiative for help with the generation of adenoviral vectors. M.S. was supported by a Schering postdoctoral fellowship, J.U. was supported by a Mildred Scheel postdoctoral fellowship and M.N. and G.W. received support from the Juvenile Diabetes Research Foundation. Support to K.H. was from the NIH Director's Innovator Award, the Harvard Stem Cell Institute, the Kimmel Foundation and the V Foundation. The authors are filing a patent based on the results reported in this paper.

Supporting Online Material

www.sciencemag.org/cgi/content/full/1162494/DC1
Materials and Methods
Figs. S1 to S10
Tables S1 to S3
References

30 June 2008; accepted 17 September 2008
Published online 25 September 2008;
10.1126/science.1162494
Include this information when citing this paper.

Generation of Mouse Induced Pluripotent Stem Cells Without Viral Vectors

Keisuke Okita,[1] Masato Nakagawa,[1,2] Hong Hyenjong,[2] Tomoko Ichisaka,[1,3] Shinya Yamanaka[1,2,3,4]*

Induced pluripotent stem (iPS) cells have been generated from mouse and human somatic cells by introducing Oct3/4 and Sox2 with either Klf4 and c-Myc or Nanog and Lin28 using retroviruses or lentiviruses. Patient-specific iPS cells could be useful in drug discovery and regenerative medicine. However, viral integration into the host genome increases the risk of tumorigenicity. Here, we report the generation of mouse iPS cells without viral vectors. Repeated transfection of two expression plasmids, one containing the complementary DNAs (cDNAs) of Oct3/4, Sox2, and Klf4 and the other containing the c-Myc cDNA, into mouse embryonic fibroblasts resulted in iPS cells without evidence of plasmid integration, which produced teratomas when transplanted into mice and contributed to adult chimeras. The production of virus-free iPS cells, albeit from embryonic fibroblasts, addresses a critical safety concern for potential use of iPS cells in regenerative medicine.

iPS cells were first generated from mouse fibroblasts by retroviral-mediated introduction of four factors, Oct3/4, Sox2, Klf4, and c-Myc (*1*). Human fibroblasts can also be reprogrammed by the same four factors (*2*–*4*) or by Oct3/4, Sox2, Nanog, and Lin28 (*5*). Mouse and human iPS cells are similar to embryonic stem (ES) cells in morphology, gene expression, epigenetic status, and in vitro differentiation. Furthermore, mouse iPS cells give rise to adult chimeras and show competence for germline transmission (*6*–*8*). However, chimeras and progeny mice derived from iPS cells frequently develop tumors, which in some cases may be due to reactivation of the c-Myc oncogene (*7*). It is possible to generate iPS cells without retroviral insertion of c-Myc (*9*, *10*), albeit at a lower efficiency. Nevertheless, retroviral integration of the other transcription factors may activate or inactivate host genes, resulting in tumorigenicity, as was the case in some patients who underwent gene therapy (*11*). In order to apply the technology to cell transplantation therapy, it is crucial to generate iPS cells with use of nonintegration methods (*12*).

To generate mouse iPS cells without retroviruses, we used an adenovirus-mediated gene delivery system. As an initial step, we generated iPS cells with one or two factors using adenoviruses and using retroviruses for the remaining factors. We used mice in which green fluorescence protein (GFP) and the puromycin-

[1]Center for iPS Cell Research and Application (CiRA), Institute for Integrated Cell-Material Sciences, Kyoto University, Kyoto 606-8507, Japan. [2]Department of Stem Cell Biology, Institute for Frontier Medical Sciences, Kyoto University, Kyoto 606-8507, Japan. [3]Core Research for Evolutional Science and Technology and Yamanaka iPS Cell Project, Japan Science and Technology Agency, Kawaguchi 332-0012, Japan. [4]Gladstone Institute of Cardiovascular Disease, San Francisco, CA 94158, USA.

*To whom correspondence should be addressed. E-mail: yamanaka@frontier.kyoto-u.ac.jp

resistant gene are driven by the *Nanog* enhancer and promoter (*7*). With the Nanog reporter, iPS cells can be selected with puromycin and detected as GFP-positive colonies. We transduced mouse primary hepatocytes from the Nanog reporter mice with combinations of retroviruses and adenoviruses. We chose hepatocytes because iPS cells derived from hepatocytes have fewer retroviral integration sites than do iPS cells derived from fibroblasts (*13*). Because transgene expression should be maintained for up to 12 days during iPS cell generation (*14*, *15*), we repeatedly delivered adenoviruses. We observed GFP-positive colonies when Sox2 or Klf4 was introduced with adenovirus and the remaining two factors–Oct3/4 and Klf4 or Oct3/4 and Sox2, respectively–were introduced with retroviruses (Fig. 1A). We confirmed that these iPS cells did not show integration of adenoviral transgenes (Fig. 1B). They expressed markers of ES cells, including Nanog, Rex1, and ECAT1, in quantities similar to those in ES cells (Fig. 1C). They formed teratomas containing derivatives of all three germ layers when transplanted subcutaneously into nude mice (Fig. 1D). No GFP-positive colonies emerged when Oct3/4 was introduced with adenoviruses and Klf4 and Sox2 with retroviruses (Fig. 1A). Furthermore, we did not obtain GFP-positive colonies upon introduction of two factors by adenoviruses.

We were unable to generate iPS cells by introducing the four factors with separate adenoviral vectors. This might be due to the inability to introduce multiple factors into the same cells at sufficient concentrations. Hence, we placed the cDNAs encoding Oct3/4, Sox2, and Klf4 into a single expression vector. To this end, we used the foot-and-mouth disease virus 2A self-cleaving peptide (*16*, *17*), which enables efficient polycistronic expression in ES cells. We first placed the three cDNAs in all possible orders into pMXs retroviral vectors (*18*) (fig. S1A). We then transduced Nanog reporter mouse embryonic fibroblasts (MEFs) with these retroviruses to induce iPS cells. We observed the highest efficiency of GFP-positive colony formation when the factors were in order as Oct3/4, Klf4, and then Sox2 (fig. S1, B and C).

Next, we placed the three factors in this same order into a plasmid vector containing the CAG constitutively active promoter (*19*) (pCX-OKS-2A, Fig. 2A). In addition, we constructed another plasmid to express c-Myc (pCX-cMyc, Fig. 2A). In the initial attempt (experiment number 432), we transfected pCX-OKS-2A on days 1 and 3 and pCX-cMyc on days 2 and 4 (Fig. 2B). We obtained GFP-positive colonies that were morphologically indistinguishable from mouse ES cells (Fig. 2C). These virus-free iPS cells expressed ES cell marker genes at levels comparable to those in ES cells (Fig. 2D) and gave rise to adult chimeric mice (Fig. 2E). These data showed that mouse iPS cells can be generated without retroviruses or lentiviruses. Polymerase chain reaction (PCR) analyses, however, detected plasmid incorporation into the host genome (Fig. 2F).

We then modified the transfection protocol in order to avoid plasmid integration. We transfected pCX-OKS-2A and pCX-cMyc together on days 1, 3, 5, and 7 (experiment number 440, Fig. 2B). We obtained multiple GFP-positive colonies, which gave rise to cells morphologically indistinguishable from ES cells (Fig. 2C). These cells expressed markers of ES cells at comparable levels (Fig. 2D). To test for genomic integration of plasmid DNA, we designed 16 sets of PCR

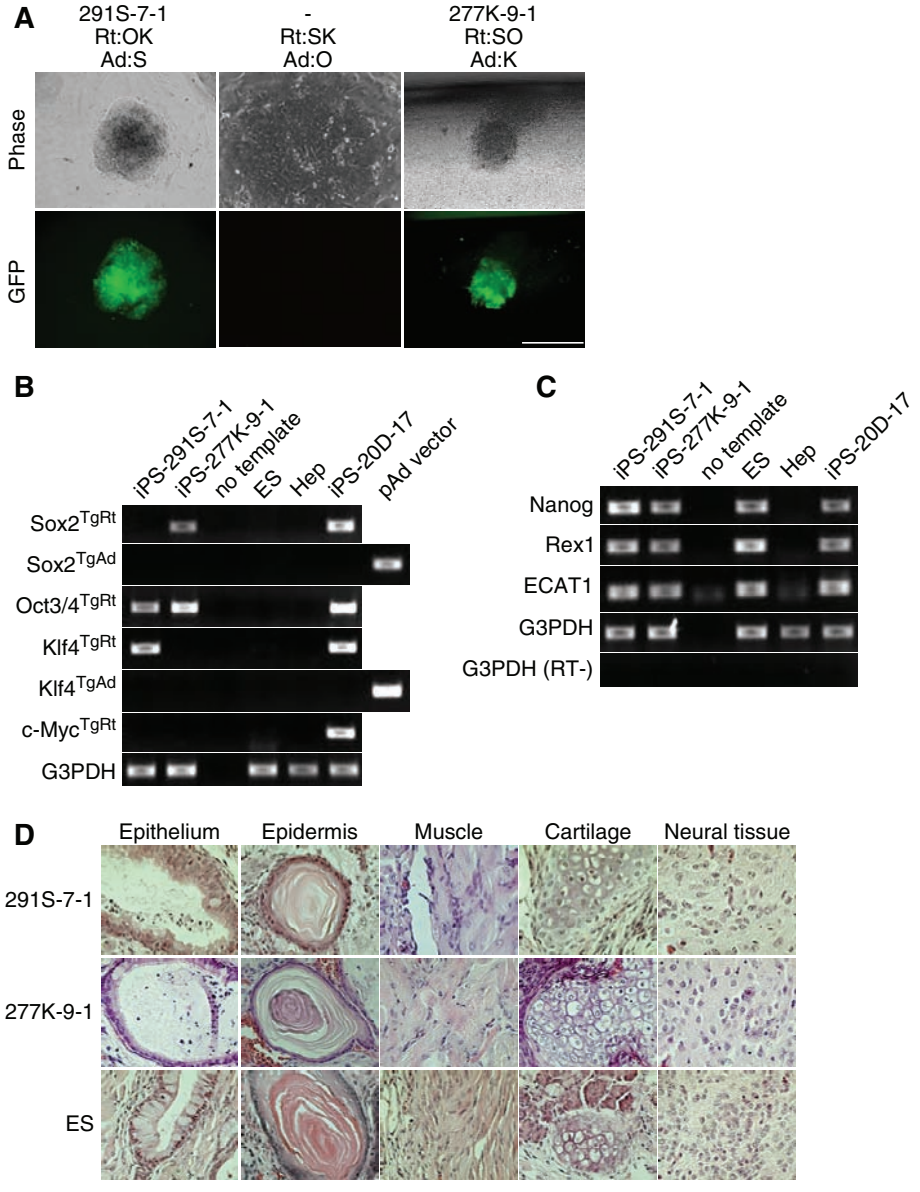

Fig. 1. Generation of iPS cells with adenovirus/retrovirus combination. (**A**) Morphology of iPS cells established by adenovirus/retrovirus combination. The iPS cell clone 291S-7-1 was generated with retroviral (Rt) introduction of Oct3/4 (O) and Klf4 (K) and adenoviral (Ad) introduction of Sox2 (S). The iPS cell clone 277K-9-1 was generated with retroviral introduction of Oct3/4 and Sox2 and adenoviral introduction of Klf4. Scale bar indicates 500 μm. (**B**) Integration of retroviral transgenes (TgRt) and adenoviral transgenes (TgAd) of the four factors was examined by genomic PCR analyses. As a control of TgRt, iPS cells generated with retroviruses (clone 20D-17) were used. As a control of TgAd, the plasmid pAd/CMV/V5-DEST vectors containing Sox2 or Klf4 were used. ES, RF8 mouse ES cells; Hep, mouse primary hepatocytes. As a loading control, the housekeeping gene, glyceraldehyde-3-phosphate dehydrogenase (G3PDH) was used. (**C**) Reverse transcription PCR (RT-PCR) analyses of ES cell marker genes and transgenes in RF8 mouse ES cells and iPS cells (clones 291S-7-1, 277K-9-1, and 20D-17). As a loading control, G3PDH was used. As a negative control, G3PDH was amplified without the reverse transcriptase (RT–). (**D**) Teratoma formation. RF8 ES cells or iPS cells (clones 291S-7-1 and 277K-9-1) were subcutaneously transplanted into nude mice. After 4 weeks, tumors were sectioned and stained with hematoxylin and eosin staining. Shown are gutlike epithelial tissues (left), epidermal tissues, striated muscles, cartilage, and neural tissues (right).

primers to amplify various parts of the plasmids (Fig. 2A). In 9 out of 11 GFP-positive clones obtained by the modified protocol, no amplification of plasmid DNA was observed (Fig. 2F). In addition, Southern blot analyses did not detect integration of transgenes in these clones (fig. S2). Although we cannot formally exclude the presence of small plasmid fragments, these data show that the iPS cells are most likely free from plasmid integration into the host genome.

To exclude the possibility that virus-free iPS cells were derived from contamination of Nanog reporter ES cells that we have in our laboratory, we performed simple sequence length polymorphisms (SSLP) analyses. In experiment number

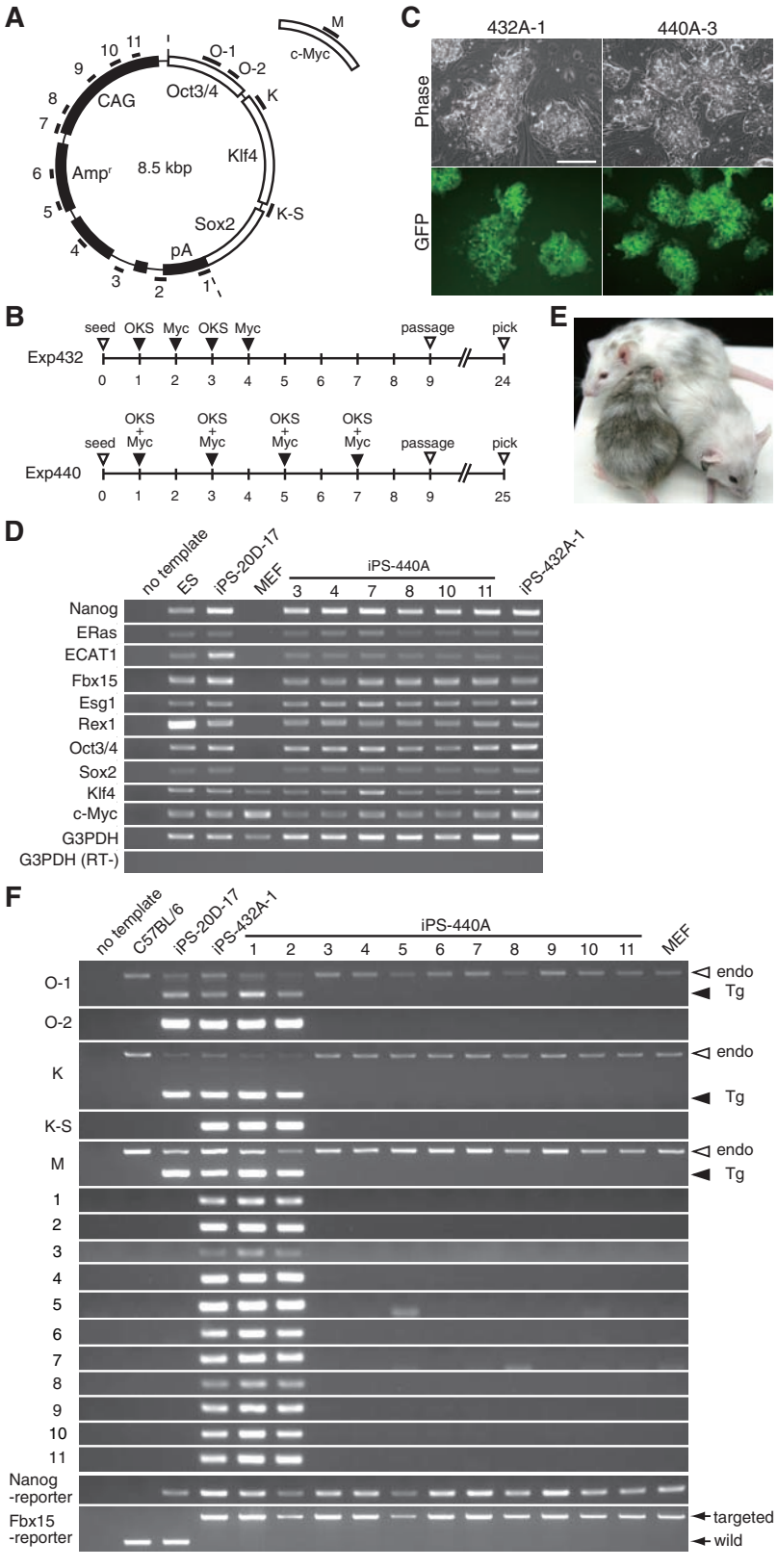

Fig. 2. Generation of virus-free iPS cells. (**A**) Expression plasmids for iPS cell generation. The three cDNAs encoding Oct3/4, Klf4, and Sox2 were connected in this order with the 2A peptide and inserted into the pCX plasmid (pCX-OKS-2A). In addition, the c-Myc cDNA was inserted into pCX (pCX-cMyc). Thick lines (O-1, O-2, K, K-S, 1 to 11, and M) indicate amplified regions used in (F) to detect plasmid integration into genome. The locations of the CAG promoter, the ampicillin-resistant gene (Amp^r), and the polyadenylation signal (pA) are also shown. (**B**) Time schedules for induction of iPS cells with plasmids. Open arrowheads indicate the timing of cell seed, passage, and colony pickup. Solid arrowheads indicate the timing of transfection. (**C**) Colonies of virus-free iPS cells. Scale bar, 200 μm. (**D**) Gene expression. Total RNAs isolated from ES cells, retrovirus-induced iPS cells (clone 20D-17), plasmid-induced iPS cells (clones 440A-3, -4, -7, -8, -10, and -11 and clone 432A-1), and MEFs were analyzed with RT-PCR. (**E**) Chimeric mice derived from the clone 432A-1. (**F**) Detection of plasmid integration by PCR. Genomic DNA from a C57BL/6 mouse, retrovirus-induced iPS cells (clone 20D-17), plasmid-induced iPS cells (clone 432A-1 and clones 440A-1 to -11), and MEFs were amplified by PCR with primers indicated in (A). In PCR for O-1, K, and M, bands derived from the endogenous (endo) genes are shown with open arrowheads, whereas those from integrated plasmids (Tg) shown with solid arrowheads. For the Fbx15 reporter, the lower bands indicate the wild-type allele, whereas the upper bands indicate the knock-in allele. Minor PCR bands seen in some virus-free clones are smaller than expected and are most likely derived from primer dimers.

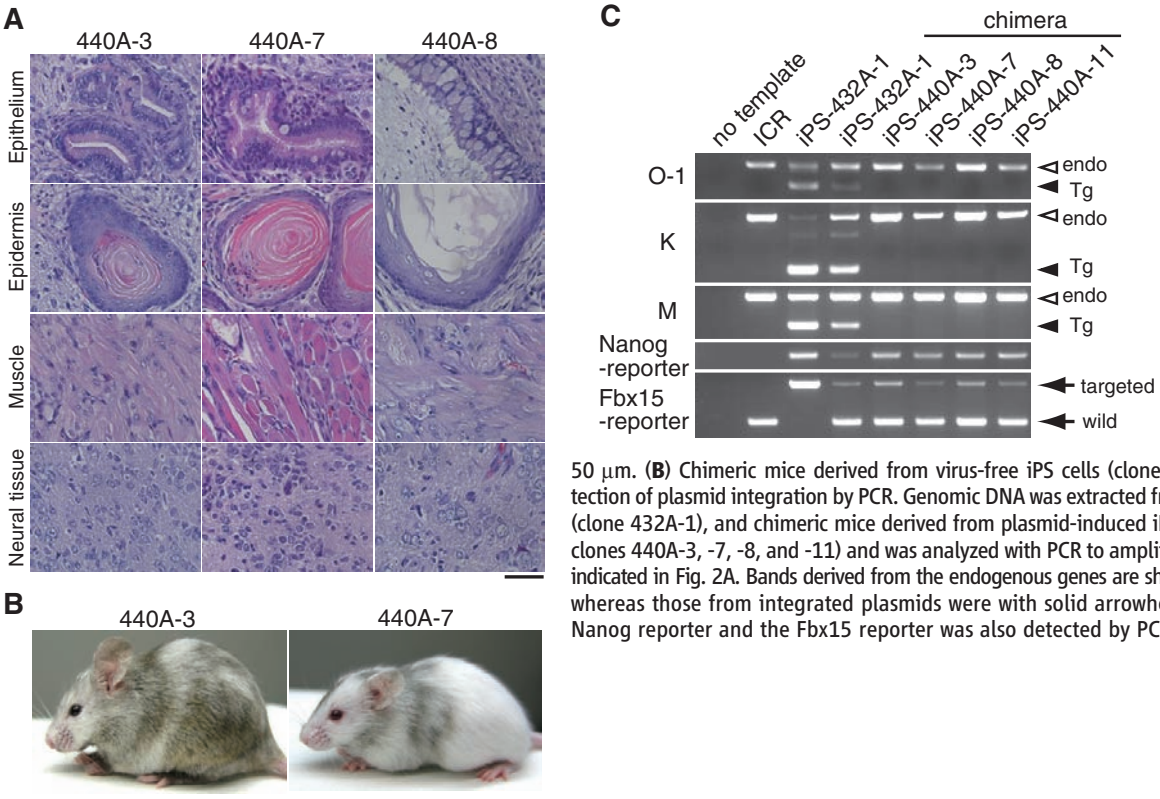

Fig. 3. Pluripotency of virus-free iPS cells without evidence of transgene integration. (**A**) Teratoma formation. Virus-free iPS cells (clones 440A-3, -7, and -8) were subcutaneously transplanted into nude mice. After 4 weeks, tumors were sectioned and stained with hematoxylin and eosin staining. Shown are gutlike epithelial tissues (upper), epidermal tissues, striated muscles, and neural tissues (bottom). Scale bar, 50 μm. (**B**) Chimeric mice derived from virus-free iPS cells (clones 440A-3 and -7). (**C**) Detection of plasmid integration by PCR. Genomic DNA was extracted from an ICR mouse, iPS cells (clone 432A-1), and chimeric mice derived from plasmid-induced iPS cells (clone 432A-1 and clones 440A-3, -7, -8, and -11) and was analyzed with PCR to amplify fragments O-1, K, and M indicated in Fig. 2A. Bands derived from the endogenous genes are shown with open arrowheads, whereas those from integrated plasmids were with solid arrowheads. The presence of the Nanog reporter and the Fbx15 reporter was also detected by PCR.

440, we used MEFs derived from five mouse embryos. SSLP analyses were able to distinguish these five and identified the origin of each virus-free iPS cells. The analyses also confirmed that virus-free iPS cells are different from ES cells, the latter of which were derived from the mouse strain 129S4 (fig. S3).

We performed 10 independent experiments with this transfection protocol (table S1). In 7 out of the 10 experiments, we obtained GFP-positive colonies. In these experiments, 1 to 29 GFP-positive colonies emerged from 1×10^6 transfected cells. When we used retroviruses, we routinely obtained >100 GFP-positive colonies with this number of transfected cells when using three factors and ~1000 GFP-positive colonies with the four factors. In addition, because we re-plated transfected MEFs at day 9, some virus-free iPS cell clones may derive from common progenitor cells. Thus, the efficiency of iPS cell induction with the plasmid transfection protocol is substantially lower than that with the retroviral method. Nevertheless, we obtained iPS cell clones without evidence of plasmid integration in 6 out of 10 experiments (figs. S2 to S5), demonstrating reproducibility of the protocol.

To confirm pluripotency of these iPS cells, we transplanted them subcutaneously into nude mice. All clones tested (440A-3, -4, -7, -8, -10, and -11; 492B-4 and -9; 497B-30; and 497D-2) gave rise to tumors containing a wide variety of cell types, including cells derived from all three germ layers (Fig. 3A and fig. S5). We also injected the iPS cells into blastocysts from the mouse strain ICR. From all clones injected (440A-3, -4, -6, -7, -8, -9, -10, and -11; 492B-4 and 9), we obtained adult chimeras, as judged from coat color (Fig. 3B). In these chimera mice, we did not detect integration of the transgenes by PCR (Fig. 3C). Furthermore, PCR analyses detected both the Nanog reporter and the Fbx15 reporter (*20*) in chimeras (Fig. 3C). Because we generated these virus-free iPS cells from the double reporter mice in the experiment number 440 and because we do not have double reporter ES cells in our laboratory, these data confirmed that these chimeras were derived from the virus-free iPS cells but not from contaminated ES cells. These results confirm pluripotency of iPS cells generated by plasmid transfection methods.

We previously reported that we did not find common retroviral integration sites in iPS cell derived from mouse liver and stomach (*13*). The current study shows dispensability of retroviral integration in iPS cell generation. The efficiency of iPS cell generation, however, is substantially lower without retroviruses. This may suggest that retroviral integration facilitates iPS cell generation. Alternatively, the lower efficiency may be attributable to lower transgene expression levels observed with plasmid transfection than those with retroviruses (fig. S6). Further studies are required to increase the efficiency of virus-free iPS cells. In addition, whether virus-free iPS cells are germline-competent and whether they can be generated from adult somatic cells remain to be determined. Nevertheless, our study is an important step toward studying patient-specific cells and associated disease as well as future application of iPS cell technology in regenerative medicine and other clinical usages.

References and Notes

1. K. Takahashi, S. Yamanaka, *Cell* **126**, 663 (2006).
2. W. E. Lowry *et al.*, *Proc. Natl. Acad. Sci. U.S.A.* **105**, 2883 (2008).
3. I. H. Park *et al.*, *Nature* **451**, 141 (2008).
4. K. Takahashi *et al.*, *Cell* **131**, 861 (2007).
5. J. Yu *et al.*, *Science* **318**, 1917 (2007); published online 19 November 2007 (10.1126/science.1151526).
6. N. Maherali *et al.*, *Cell Stem Cell* **1**, 55 (2007).
7. K. Okita, T. Ichisaka, S. Yamanaka, *Nature* **448**, 313 (2007).
8. M. Wernig *et al.*, *Nature* **448**, 318 (2007).
9. M. Nakagawa *et al.*, *Nat. Biotechnol.* **26**, 101 (2008).
10. M. Wernig, A. Meissner, J. P. Cassady, R. Jaenisch, *Cell Stem Cell* **2**, 10 (2008).
11. A. W. Nienhuis, C. E. Dunbar, B. P. Sorrentino, *Mol. Ther.* **13**, 1031 (2006).
12. S. Yamanaka, *Cell Stem Cell* **1**, 39 (2007).
13. T. Aoi *et al.*, *Science* **321**, 699 (2008); published online 12 February 2008 (10.1126/science.1154884).
14. T. Brambrink *et al.*, *Cell Stem Cell* **2**, 151 (2008).
15. M. Stadtfeld, N. Maherali, D. T. Breault, K. Hochedlinger, *Cell Stem Cell* **2**, 230 (2008).
16. E. C. Hsiao *et al.*, *PLoS One* **3**, e2532 (2008).
17. K. Hasegawa, A. B. Cowan, N. Nakatsuji, H. Suemori, *Stem Cells* **25**, 1707 (2007).
18. S. Morita, T. Kojima, T. Kitamura, *Gene Ther.* **7**, 1063 (2000).
19. H. Niwa, K. Yamamura, J. Miyazaki, *Gene* **108**, 193 (1991).
20. Y. Tokuzawa *et al.*, *Mol. Cell. Biol.* **23**, 2699 (2003).

21. We thank K. Takahashi, K. Yae, M. Koyanagi, and K. Tanabe for scientific discussion; K. Okuda, M. Narita, A. Okada, H. Miyachi, S. Kitano, and N. Takizawa for technical assistance; R. Kato, R. Iyama, E. Nishikawa, and Y. Shimazu for administrative assistance; and D. Srivastava for critical reading of the manuscript. We also thank J. Miyazaki for the CAG promoter,

T. Kitamura for Plat-E cells and pMXs retroviral vectors, and R. Farese for RF8 ES cells. This study was supported in part by a grant from the Program for Promotion of Fundamental Studies in Health Sciences of National Institute of Biomedical Innovation (NIBIO), a grant from the Leading Project of Ministry of Education, Culture, Sports, Science, and Technology (MEXT), a grant from Uehara Memorial Foundation, and grants-in-aid for scientific research of Japan Society for the Promotion of Science (JSPS) and MEXT (to S.Y.). K.O. was a JSPS research fellow. H.H. is supported by a Japanese government (MEXT) scholarship. The authors are filing a patent based on the results reported in this paper.

Supporting Online Material
www.sciencemag.org/cgi/content/full/1164270/DC1
Materials and Methods
Figs. S1 to S6
Tables S1 and S2

6 August 2008; accepted 25 September 2008
Published online 9 October 2008;
10.1126/science.1164270
Include this information when citing this paper.

Insights into Translational Termination from the Structure of RF2 Bound to the Ribosome

Albert Weixlbaumer,* Hong Jin,* Cajetan Neubauer, Rebecca M. Voorhees, Sabine Petry,† Ann C. Kelley, Venki Ramakrishnan‡

The termination of protein synthesis occurs through the specific recognition of a stop codon in the A site of the ribosome by a release factor (RF), which then catalyzes the hydrolysis of the nascent protein chain from the P-site transfer RNA. Here we present, at a resolution of 3.5 angstroms, the crystal structure of RF2 in complex with its cognate UGA stop codon in the 70*S* ribosome. The structure provides insight into how RF2 specifically recognizes the stop codon; it also suggests a model for the role of a universally conserved GGQ motif in the catalysis of peptide release.

In nearly all species, three stop codons, UGA, UAG, and UAA, signal the end of the coding sequence in mRNA. These stop codons are decoded by a protein factor termed a class I release factor (RF) (*1*, *2*). In bacteria, there are two such factors with overlapping specificity: RF1 recognizes UAG, RF2 recognizes UGA, and both recognize UAA. In eukaryotes, a single RF, eRF1, recognizes all three stop codons. The mechanism by which RFs specifically decode stop codons and catalyze peptidyl-tRNA hydrolysis is a fundamental problem in understanding translation.

Elements of RFs involved in catalysis and stop-codon recognition have been proposed, using sequence analysis combined with biochemistry and genetics. A universally conserved tripeptide sequence, GGQ (*3*), has been implicated in the hydrolysis of the peptide chain from tRNA (*4*). Exchanging a tripeptide motif between RF1 and RF2 [P(A/V)T in RF1; SPF in RF2] switches their respective specificities for UAG and UGA (*5*). Hydroxyl-radical probing suggested that the SPF and GGQ motifs were close to the decoding center and peptidyl transferase center (PTC), respectively (*6*).

The structure of the eukaryotic eRF1 suggested that the distance between its codon-recognition and GGQ motifs was compatible with the approximately 75 Å distance between the decoding center and the PTC (*7*). However, eRF1 has no sequence or structural homology to bacterial RFs. The crystal structure of a bacterial RF2 (*8*) showed that the distance between the SPF and GGQ motifs was about 23 Å and thus incompatible with their simultaneous involvement in decoding and peptide release. This anomaly was resolved when low-resolution structures (*9*–*11*) showed that the conformation of RF2 when bound to the ribosome was different, so that the GGQ and SPF/PVT motifs were localized to the PTC and decoding center, respectively. However, the resolution of these

Medical Research Council (MRC) Laboratory of Molecular Biology, Hills Road, Cambridge CB2 0QH, UK.

*These authors contributed equally to this work.
†Present address: Department of Cellular and Molecular Pharmacology, University of California, San Francisco, 600 16th Street, San Francisco, CA 94158-2517, USA.
‡To whom correspondence should be addressed. E-mail: ramak@mrc-lmb.cam.ac.uk

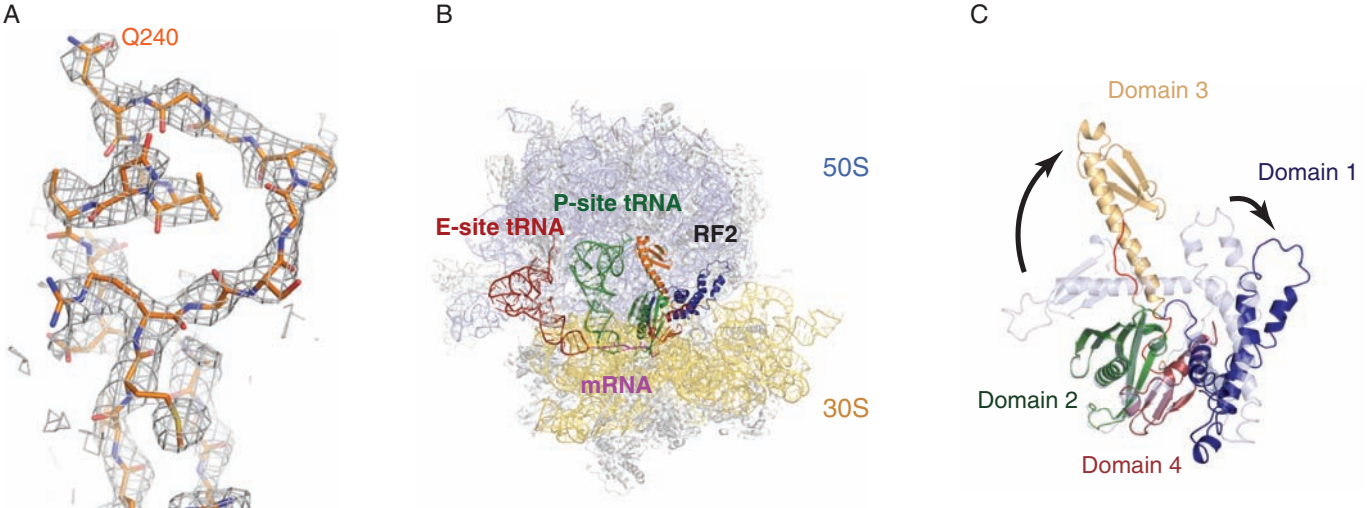

Fig. 1. The structure of RF2 in the ribosome. (**A**) Unbiased difference Fourier maps showing the density of RF2 in the peptidyl transferase center of the ribosome. (**B**) Overview of the structure showing the 50*S* subunit (light blue), the 30*S* subunit (yellow) with E-site tRNA (red), P-site tRNA (green), and RF2 colored by domains as in (**C**). The mRNA is shown in magenta. (**C**) Conformational differences between the isolated crystal structure of RF2 (*15*) (shown in light blue), and the ribosome-bound form (colored by domains as labeled) are indicated. Loop regions connecting domain 3 with domains 2 and 4, that undergo substantial conformational changes, are highlighted in red.